


ORIGINAL ARTICLE

Tau Pathology in Chronic Traumatic Encephalopathy is Primarily Neuronal

Morgane L.M.D. Butler, BSc, Erin Dixon, BS, Thor D. Stein, MD, PhD, Victor E. Alvarez, MD, Bertrand Huber, MD, PhD, Michael E. Buckland, MBBS, PhD, FRCPA, FFSc, Ann C. McKee, MD, and Jonathan D. Cherry , PhD

Abstract

Millions of individuals are exposed to repetitive head impacts (RHI) each year through contact sports, military blast, and interpersonal violence. RHI is the major risk factor for developing chronic traumatic encephalopathy (CTE), a neurodegenerative tauopathy. Recent consensus criteria defined the pathognomonic lesion in CTE as perivascular, hyperphosphorylated tau (p-tau) in neuronal aggregates. Astroglial p-tau is an inconsistent supporting feature and not in itself diagnostic of CTE. This study quantitated the spatial and cellular distribution of p-tau pathology in postmortem dorsolateral frontal cortex

of 150 individuals with CTE, from ages 21 to 80 years old, without comorbid pathology. p-Tau-immunoreactive cells were quantitated in the gray matter sulcus, crest, subpial region, and within pathognomonic CTE lesions. Significantly more neuronal p-tau than astrocytic p-tau was found across all cortical regions ($p < 0.0001$). Sulcal astrocytic p-tau was primarily (75%, $p < 0.0001$) localized to subpial regions as thorn-shaped astrocytes, a form of age-related tau astroglialopathy. Neuronal p-tau was significantly associated with age, years of RHI exposure, and CTE severity; astrocytic p-tau pathology was only significantly associated with age. These findings strongly support neuronal degeneration as a driving feature of CTE and will help inform future research and the development of fluid biomarkers for the detection of neuronal degeneration in CTE.

Key Words: Age-related tau astroglialopathy, Chronic traumatic encephalopathy, CTE, Neurodegeneration, Neuropathology, Repetitive head impacts, Tauopathy.

From the Department of Anatomy and Neurobiology, Boston University School of Medicine, Boston, Massachusetts, USA (MLMDB, ACM); VA Boston Healthcare System, Jamaica Plain, Massachusetts, USA (MLMDB, ED, TDS, VEA, BH, ACM, JDC); Boston University Alzheimer's Disease and CTE Centers, Boston University School of Medicine, Boston, Massachusetts, USA (MLMDB, ED, TDS, VEA, BH, ACM, JDC); National Center for PTSD, VA Boston Healthcare System, Boston, Massachusetts, USA (VEA, BH, ACM); VA Bedford Healthcare System, Bedford, Massachusetts, USA (TDS, VEA, BH, ACM); Department of Neuropathology, Royal Prince Alfred Hospital, Sydney, NSW, Australia (MEB); Brain and Mind Centre, University of Sydney, Camperdown, NSW, Australia (MEB); Department of Pathology and Laboratory Medicine, Boston University School of Medicine, Boston, Massachusetts, USA (TDS, JDC); Department of Neurology, Boston University School of Medicine, Boston, Massachusetts, USA (ACM, JDC).

Send correspondence to: Jonathan D. Cherry, PhD, VA Boston Healthcare System, 150 S. Huntington Ave., Boston, MA 02130, USA; E-mail: jdcherry@bu.edu

This work was supported by grant funding from the NIH (U19-AG068753, AG08122, and AG054076), the NIA (AG057902, AG06234, RF1AG054156, and RF1AG057768), the NINDS (U54NS115266 and U01NS086659), the National Institute of Aging Boston University AD Center (P30AG072978), Department of Veterans Affairs Biorepository (BX002466), Department of Veterans Affairs Merit Award (101-CX001038), Department of Veterans Affairs Career Development Award (BX004349), and the Nick and Lynn Buoniconti Foundation. The views, opinions, and/or findings contained in this article are those of the authors and should not be construed as an official Veterans Affairs or Department of Defense position, policy, or decision unless so designated by other official documentation. Funders did not have a role in the design and conduct of the study; collection, management, analysis, and interpretation of the data; preparation, review, or approval of the manuscript; or decision to submit the manuscript for publication.

The authors have no duality or conflicts of interest to declare.

INTRODUCTION

Chronic traumatic encephalopathy (CTE) is a progressive neurodegenerative disease associated with a history of exposure to repetitive head impacts (RHI) sustained through contact sports, such as American football, hockey, soccer, and boxing, military service, or interpersonal violence (1, 2). Currently, CTE can only be diagnosed after death, and there are no therapeutic treatments or interventions available. CTE is neuropathologically defined by the accumulation of hyperphosphorylated tau (p-tau) around small blood vessels and concentrated at the depths of the cortical sulcus. In early-stage CTE, tau pathology is confined to the cortical gray matter, but as the disease progresses, p-tau pathology is also observed in medial temporal lobe structures, such as the hippocampus, entorhinal cortex, amygdala, the diencephalon, and brainstem (3). The 2015 CTE consensus conference defined the pathognomonic lesion as “an abnormal accumulation of p-tau in neurons and astrocytes distributed around small blood vessels at the depth of the cortical sulcus in an irregular pattern” (4). The revised 2021 CTE consensus criteria state that “a pathognomonic lesion consists of p-tau aggregates in neurons with or without glial tau at the depth of a cortical sulcus around a small blood vessel” (3, 5),

highlighting that p-tau containing neurons (i.e. neurofibrillary tangles [NFTs], pretangles, and neurites) are the primary p-tau containing cell type observed in CTE. Furthermore, our previous analysis of 99 contact sport athletes diagnosed with CTE with no comorbidities, ranging in age at death from ages 20 to 89, found that the presence of p-tau containing astrocytes within the pathognomonic CTE lesion seemed to be associated with age at death and that most p-tau containing cells in the CTE pathognomonic lesions were neurons (6). However, this previous analysis was restricted to morphologic assessment. New techniques and methods that utilize machine learning and artificial intelligence platforms to count cells are superior. Additionally, to truly identify cell population that contains p-tau, multiplex immunofluorescence labeling (mIF) is required.

Subtypes of astrocytic p-tau have been described principally using morphologic assessment of p-tau-immunolabeled histological sections (7). Tufted astrocytes are hallmarks of progressive supranuclear palsy (8); astrocytic plaques are found in corticobasal degeneration (9); ramified astrocytes are present in Pick disease (8); and globular astroglial inclusions are seen in globular glial tauopathy (7). Astrocytic pathology that is related to brain aging is broadly termed age-related tau astroglial pathology (ARTAG) and includes the thorn-shaped astrocytes and granular-fuzzy astrocytes that can be found in the white and gray matter, and in subpial, subependymal, and perivascular locations (7). ARTAG pathology is typically observed in individuals over the age of 60 years old and due to its subpial and perivascular localization can sometimes be confused with CTE (7). The 2021 consensus criteria for CTE clarified that subpial TSA pathology, or ARTAG, is not a diagnostic feature of the CTE pathognomonic lesion. Recently, however, a study of 22 aged individuals variably diagnosed with CTE, whose age range at death was narrow (most individuals over the age of 70 [16 of whom were diagnosed with a comorbid neurodegenerative disease]), suggested that astrocytes, not neurons, better define CTE pathology (10). Further, another study of 12 aged individuals (most individuals >70 years old) diagnosed with CTE and other comorbid neurodegenerative diseases suggested that labeling of astrocytes facilitates the diagnosis of CTE (11). Both of these studies called for a revision of the NINDS CTE criteria to include astrocytic p-tau pathology in the pathognomonic lesion of CTE. To further inform this debate, we undertook a comprehensive, quantitative analysis of p-tau-positive cells in CTE in a large cohort of brain donors, representing a wide age range at death and with no comorbid neurodegenerative conditions, using mIF and cell-type specific markers. The goal was to determine the role of astrocytic p-tau pathology in the progression of CTE.

Overall, determining the spatial, temporal, and cellular distribution of p-tau deposition in CTE over the lifespan is critical to understanding the pathogenesis of CTE, and identifying novel biomarkers and therapeutic intervention strategies.

MATERIALS AND METHODS

Participant Selection and Neuropathologic Assessment

Cases were selected from the BU CTE Brain Bank. At the time of the study, there were approximately 1200 cases

that were donated to the CTE brain bank. Each donated case is assessed by a board-certified neuropathologist for a neuropathologic diagnosis of CTE, Alzheimer's disease, neocortical Lewy bodies, frontotemporal lobar degeneration, or motor neuron disease, based on established neuropathologic criteria for each disease (3, 4, 12–15). Cases were excluded if they carried a neuropathologic diagnosis of any neuropathologic disease, except CTE. Additionally, to minimize confounding effects of neuritic plaque pathology, cases were excluded if they received an amyloid beta CERAD score (Consortium to Establish a Registry for Alzheimer's Disease, semiquantitative neuritic plaque score) >1. Using these exclusion criteria, 235 cases were neuropathologically diagnosed with CTE without the presence of any other comorbid neurodegenerative disease diagnosis. Of the 235, 81 had missing tissue regions or were not immediately available for use, and 4 did not have sufficient clinical exposure records, leaving 150 available for analysis as represented in Table 1. A randomized representative subset of 51 individuals from the initial groups was used for mIF analysis. Neuropathologic diagnosis was obtained from formalin-fixed paraffin-embedded tissue as previously described (1, 4). Briefly, sections of paraffin-embedded tissue were stained for p-tau, alpha-synuclein, amyloid beta, TAR DNA-Binding Protein-43 (TDP-43), Luxol fast blue, and hematoxylin and eosin using previously described methods (16). A neuropathologic diagnosis of CTE was made using National Institute of Neurological Disorders and Stroke (NINDS) / National Institute of Biomedical Imaging and Bioengineering (NIBIB) consensus criteria (3, 4). Individuals with CTE were diagnosed based on the presence, extent, and severity of p-tau deposition through the brain. All evaluations were reviewed by 4 neuropathologists (VEA, BH, TDS, and ACM); discrepancies in the diagnosis were resolved by a consensus conference. Demographics, athletic history (type of sports played, level, position, age of first exposure to sports, and years playing contact sports), military history (branch, location of service, and duration of combat exposure), and traumatic brain injury history (including the number of concussions) were queried during a telephone interview, as detailed previously (17). Institutional review board approval for brain donation was obtained through the Boston University Alzheimer's Disease and CTE Center, Human Subjects Institutional Review Board of the Boston University School of Medicine, and VA Bedford Healthcare System (Bedford, MA). One individual from the Australian Sports Brain Bank was used for a representative image in Figure 3 but not included in the data analysis. The Australian Sports Brain Bank operates under RPA Human Research Ethics Committee approval X19-0010.

Immunohistochemistry and Immunofluorescence Staining

Tissue was obtained from the dorsolateral frontal cortex (DLFC) and processed as previously described (18). The DLFC was chosen because it is one of the first regions affected in CTE. Since pathologic alterations are found in the DLFC early, it is easier to identify more subtle changes and observe a

TABLE 1. Group Demographics

| | | CTE I | CTE II | CTE III | CTE IV | Total/Mean | |
|--|-------|-------------|-------------|-------------|-------------|-------------|-----------|
| n | (IHC) | 16 | 57 | 62 | 15 | 150 | |
| | (IF) | 4 | 14 | 27 | 6 | 51 | |
| Age at death (years) | (IHC) | 39.6 ± 18.4 | 41.8 ± 14.3 | 60.7 ± 12.4 | 70.4 ± 9.6 | 52.2 ± 17.5 | p < 0.001 |
| | (IF) | 28.3 ± 2.1 | 41.4 ± 12.2 | 57.8 ± 12.0 | 68.3 ± 10.4 | 52.2 ± 15.9 | |
| Contact sports exposure (years) | (IHC) | 13.1 ± 3.4 | 16.5 ± 8.4 | 17.0 ± 5.2 | 21.5 ± 9.7 | 16.9 ± 7.2 | p = 0.01 |
| | (IF) | 14.5 ± 4.5 | 16.9 ± 8.5 | 17.0 ± 5.5 | 19.8 ± 7.0 | 17.1 ± 6.5 | |

Data expressed as mean ± standard deviation. Age at death and years of exposure analyzed with one-way ANOVA.

wider range of CTE-related effects. All cases used in this study had p-tau pathology in the DLFC. Both brightfield immunohistochemistry (IHC) staining and mIF were performed. Ten-micrometer thick sections were stained with anti-Phospho-Tau Ser202, Thr205 (AT8) (Invitrogen, Waltham, MA, 1:500) and visualized for IHC with 3,3'-diaminobenzidine (DAB), as previously described (18). mIF staining was performed using the Akoya Bioscience Opal Polaris 7 color manual IHC detection kit per the manufacturer's protocol and as previously described (19). Sections were incubated with antibodies to AT8 (Invitrogen, 1:500, Mouse, cat # MN1020), microtubule associated protein 2 (MAP2) (BioLegend, San Diego, CA, 1:500, Mouse, cat # 801801), and glial fibrillary acidic protein (GFAP) (BioLegend, 1:750, mouse, cat # 837604) and stained with DAPI to label cell nuclei. Sections were imaged using an Akoya Bioscience Vectra Polaris Digital Slide Scanner. Automated spectral unmixing algorithms were created using inForm software (Akoya Biosciences, Marlborough, MA) and applied to whole-slide scans in order to remove tissue autofluorescence and spectral overlap. Images were analyzed with HALO image processing software (Indica Laboratory, Albuquerque, NM).

Image Analysis

The gray matter of the depths of the cortical sulci (bottom third of two connecting gyri) and crests of the gyri (top third of the gyrus adjacent to the selected sulcus) were defined and annotated in HALO (Indica Laboratory). The gray/white matter boundary was used as the outer edge of the annotation region. Initial counting of NFTs and p-tau-positive astrocytes was carried out by morphologic assessment using IHC-stained AT8-labeled sections. All counting was performed in HALO. The sulcus and crest were annotated and analyzed separately as previously described (18). First, using HALO AI (Indica Laboratory), an image recognition algorithm was trained to identify and count NFTs. The algorithm was trained using 4236 individual neurons and allowed to iterate over 75,000 times. As astrocytes have a diverse morphologic phenotype, automated AI-based counting techniques were not able to reliably and consistently identify p-tau-positive astrocytes. Therefore, they were manually counted by an unbiased, blinded observer as previously described (6). Briefly, these cells were defined as granular, less-defined cytoplasmic p-tau staining accompanied by delicate radially oriented processes surrounding a small nucleus.

Cells that were morphologically ambiguous were not counted. Cell counts were standardized to area measured and were presented as p-tau-positive cells/mm², log of cell density, or percent of total cells. For mIF section analysis, the sulcus and crest were annotated using the same methods as the IHC analysis. Additionally, subpial regions were annotated using the HALO marginal partitioning tool and defined as the 200-µm strip of tissue below the pial surface. Lesions were identified with the help of a neuropathologist and annotated with the ellipse tool and defined as 0.4 µm² of pathognomonic CTE lesions surrounding small cortical blood vessels. This size captured lesion-associated cells, while avoiding neighboring AT8-positive cells. All lesions observed were included in the analysis. Of the 51 total mIF cases, CTE lesions were identified in 17 cases and 38 total lesions were sampled for analysis. If multiple lesions were identified within an individual, the number of cells was averaged across lesions for that one case. The total number of cells double positive for MAP2/AT8 (neurons) and GFAP/AT8 (astrocytes) were manually counted by a blinded observer and expressed either as the number of double positive cells or standardized to the total annotation area and expressed as cells/mm².

Statistics

Statistical analysis was performed using Prism (v9, GraphPad Software, San Diego, CA) or SPSS (v27). Individuals were either partitioned into groups based on CTE stage (CTE I/II/III/IV) or CTE severity [low CTE (CTE I/II) or high CTE (CTE III/IV)]. One-way ANOVA used to determine group differences in age at death and years of RHI exposure. Paired t-test was used to determine the difference between NFT- and p-tau-positive astrocyte densities. Linear regressions were used on log-transformed data to determine the relationship between p-tau containing cell densities and RHI exposure. Analyses examining associations with RHI exposure included only individuals with football as their primary method of exposure to control for differences in exposure type. Linear regression was also used to determine the relationship between percentages of p-tau containing cells in CTE lesions and age. Analysis of covariance (ANCOVA) tests were used to determine the relationship between astrocytic p-tau, NFT densities, CTE stage, and years of RHI exposure with age as a covariate.

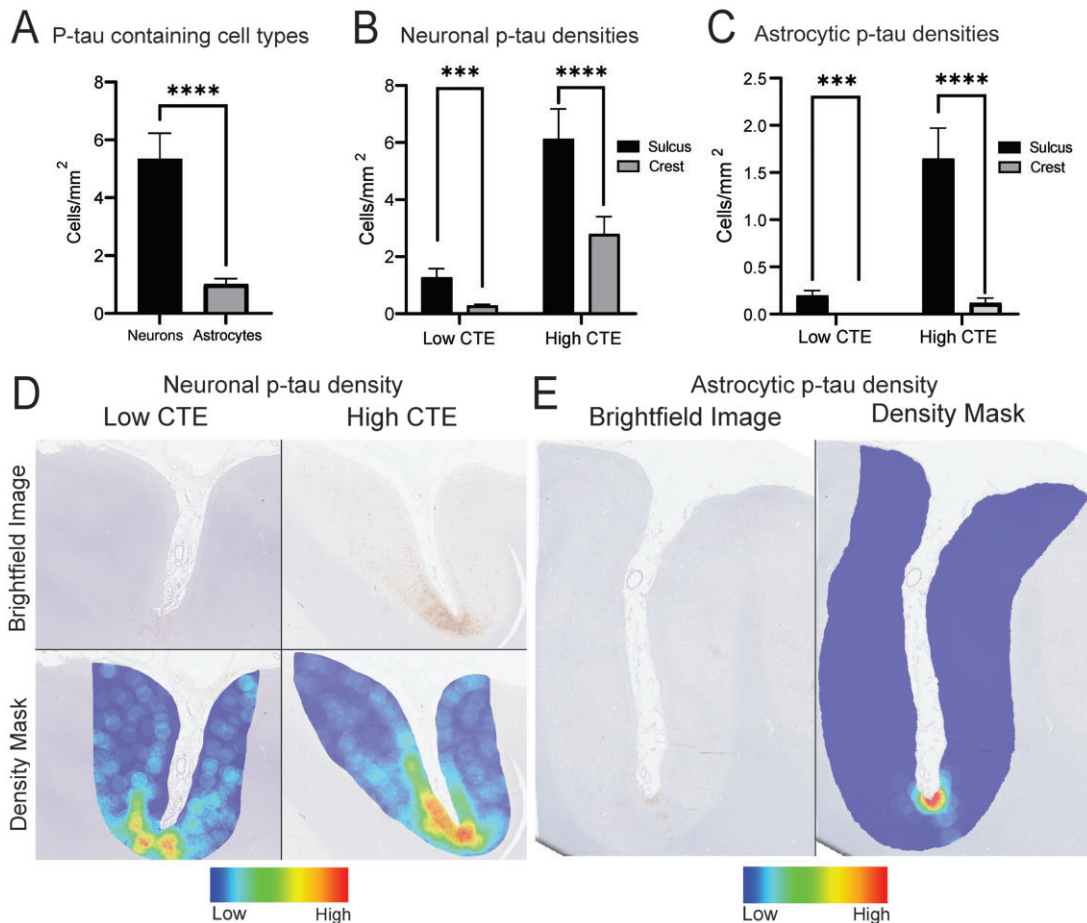


FIGURE 1. Neuronal p-tau is predominant in CTE and both neuronal and astrocytic p-tau are elevated in the sulcus. **(A)** Quantitation of all morphologically identified neurofibrillary tangles (NFTs) and p-tau containing astrocytes. Paired t-test ($****p < 0.0001$). **(B)** Neuronal p-tau densities are elevated in the sulcus in low and high CTE. Paired t-tests ($***p < 0.001$, $****p < 0.0001$). **(C)** Astrocytic p-tau densities are predominant in sulci in low and high CTE. Paired t-tests ($***p < 0.001$, $****p < 0.0001$). **(D, E)** Representative brightfield images of AT8-immunolabeled sections in low and high CTE and corresponding density heatmap demonstrating sulcal predominance of neuronal and astrocytic p-tau. All graphs represent mean \pm standard error of the mean.

RESULTS

Neuronal p-Tau is Predominant in CTE and Both Neuronal and Astrocytic p-Tau Are Elevated in the Sulcus

To examine the spatial and cellular distribution of p-tau-positive cells in CTE, IHC AT8 immunostaining was performed in the DLFC of 150 individuals pathologically diagnosed with CTE. NFTs and astrocytes were counted in the sulcus and crest from each individual. p-Tau-positive cells were found to be predominantly neuronal (Fig. 1A). NFT density was significantly elevated in the cortical sulcus compared to the gyral crest in low-stage CTE ($p < 0.0001$) and high-stage CTE (Fig. 1B, $p < 0.0001$). Additionally, there was significantly elevated sulcal astrocytic p-tau density in both low ($p < 0.001$) and high CTE ($p < 0.0001$, Fig. 1C). Density heatmap plots of the total p-tau containing neurons and astrocytes demonstrated that both cell types were found predominantly

in the sulcus compared to the crest, however, the distribution within the gray matter and prevalence differed between cell types (Fig. 1D, E).

Astrocytic p-Tau in CTE is Primarily Age-Related and Subpial, While Neuronal p-Tau Is Associated With RHI Exposure

Next, the relationship between p-tau containing cell types and age and years of RHI exposure was determined. Linear regression demonstrated that neuronal p-tau and astrocytic p-tau were both associated with age ($p < 0.0001$, $\beta = 0.343$, $p = 0.0014$, $\beta = 0.324$, Fig. 2A). However, only neuronal p-tau densities were associated with years of exposure to American football play ($p = 0.0005$, $\beta = 0.199$); astrocytic densities were not ($p = 0.329$, $\beta = 0.094$, Fig. 2B).

In order to provide a robust measure of p-tau containing cell types in CTE, mIF analysis was performed in a subset of

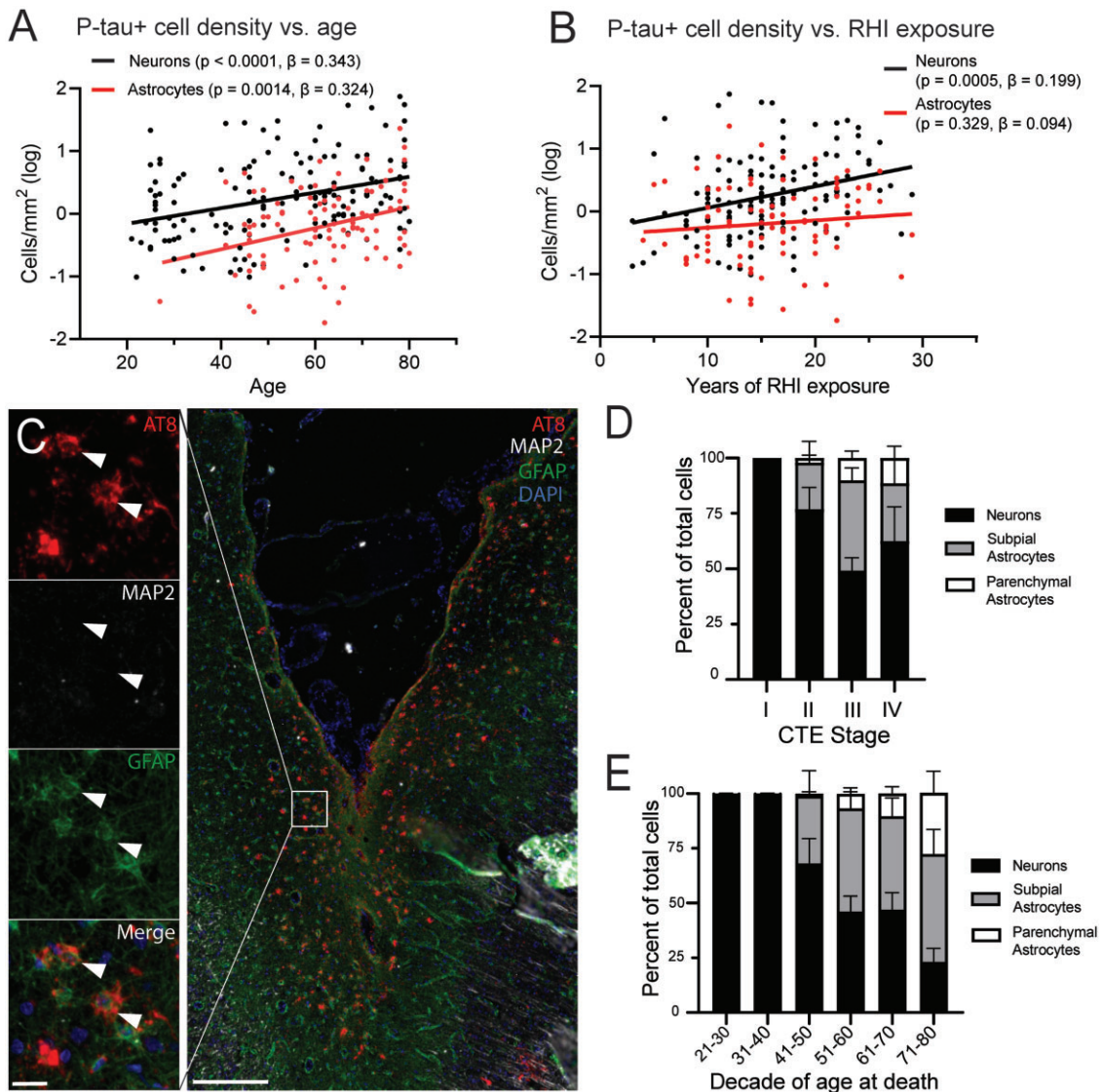


FIGURE 2. Astrocytic p-tau in CTE is primarily age-related and subpial, while neuronal p-tau is associated with RHI exposure. **(A)** Scatter plot of the log-transformed neuronal and astrocytic p-tau densities compared to age demonstrate a linear relationship between age and neuronal p-tau density ($p < 0.0001$, $\beta = 0.343$) and astrocytic p-tau density ($p = 0.0014$, $\beta = 0.324$), $n = 149$. **(B)** Comparison of log-transformed neuronal and astrocytic p-tau densities and years of RHI exposure demonstrate an association between neuronal ($p = 0.0005$, $\beta = 0.199$) but not astrocytic p-tau density ($p = 0.329$, $\beta = 0.094$) with years of RHI exposure. Only individuals who played American football were used for the RHI exposure analysis, $n = 137$. **(C)** Representative image of AT8, MAP2, and GFAP immunolabeling, left row, top to bottom. Right panel showing representative image of subpial astrocytic p-tau in a 69-year-old individual with high-stage CTE. White box indicates inset of left column, white arrows indicate cells with GFAP and AT8 colocalization. Scale bar = 10 μm and 250 μm . **(D, E)** Percentage of neuronal, subpial astrocytic, and parenchymal astrocytic p-tau densities separated by CTE stage **(D)** and decade of age **(E)** demonstrating the association of astrocytic p-tau with age but not CTE stage. Bar graphs represent mean \pm standard error of the mean.

the larger groups used for IHC analysis. Neurons were labeled with MAP2, astrocytes with GFAP, and p-tau with AT8 (Fig. 2C). To investigate the localization of p-tau containing cells within the sulcus, the sulcus was separated into parenchymal and subpial regions. Paired t-test demonstrated that a significant proportion (75.25%, $p < 0.0001$) of p-tau-positive astrocytes was localized to the subpial region (Fig. 2C).

ANCOVA analyses comparing astrocytic p-tau densities to CTE stage with age as a covariate showed that astrocytic p-tau was significantly associated with age at death ($p = 0.007$) but not CTE stage or severity ($p = 0.44$, $p = 0.105$). Subpial TSAs were observed in individuals with CTE stage II and higher, with no p-tau-positive astrocytes found in CTE stage I individuals (Fig 2D). There was no significant association between

subpial and parenchymal astrocytic p-tau densities and CTE stage (Fig. 2D). In contrast, both subpial and parenchymal astrocytic p-tau consistently increased and were significantly associated with age ($p < 0.001$, $p = 0.048$). Sparse subpial TSAs were found in one individual as young as 36 years old and were found in all cases over the age of 50. Their prevalence remained a consistent proportion of the total p-tau pathology in individuals above the age of 50. Parenchymal p-tau-positive astrocytes were present in individuals as young as 30 (one p-tau-positive astrocyte), in all cases over the age of 60, and their prevalence increased with each decade of age (Fig. 2E).

Neuronal Tau Defines the CTE Perivascular Lesion

Next, analysis was focused on the CTE lesion to further characterize the primary p-tau containing cell found within the perivascular lesion. Qualitative morphological assessment demonstrated that the cell type primarily observed around the CTE lesion was neuronal (Fig. 3A, B). Multiplex immunofluorescence was used to quantitate the number of neurons (MAP2-positive) and astrocytes (GFAP-positive) within the CTE lesion (Fig. 3C). Significantly more neuronal p-tau was observed in pathognomonic lesions compared to astrocytic p-tau in all the individuals studied, with 95% of p-tau containing cells being neurons (Fig. 3D). Only 29% of pathognomonic lesions contained astrocytic p-tau. Finally, the proportion of p-tau containing cells found within CTE lesions was not found to have a significantly increased proportion of astrocytes with increasing age ($p = 0.34$, Fig. 3F). These findings demonstrate that there is a distinct neuronal predominance of p-tau within CTE lesions in individuals across a range of ages and CTE stages.

DISCUSSION

This study demonstrated that the neuron is the primary cell type with p-tau pathology within the CTE lesion and at the depth of the cortical sulcus. Although p-tau containing astrocytes were observed in individuals with CTE, they were predominantly found as subpial TSA and not primary cell components of the deeper gray matter or perivascular CTE lesions. Furthermore, astrocytic p-tau was associated with age and not years of exposure to RHI. Overall, this work supports the 2021 consensus requirement for neuronal p-tau in the pathognomonic lesion of CTE.

Past studies have attempted to determine the cellular distribution of p-tau across neurons and astrocytes in CTE neuropathology. However, these studies solely relied on morphologic assessment of p-tau staining or assumed that 4R p-tau immunostaining was astrocyte-specific (6, 10, 20). Although morphologic assessment of p-tau in the shape of neurons or astrocytes is useful, neurons and astrocytes do not always conform to traditional morphology and can be misidentified. Recent approaches utilizing 3R and 4R p-tau isoforms to distinguish neurons and astrocytes also failed to consider the evolution of neuronal p-tau from 4R to 3R isoforms throughout the progression of CTE (6, 11, 19). This study is the first to utilize quantitative mIF to directly colocalize

cell-type-specific markers in a large group of individuals with CTE, and no comorbidities over a wide age range.

Age-related diseases such as ARTAG and primary age-related tauopathy (PART) share some pathologic features with CTE. Subpial TSA pathology or ARTAG is common in CTE and bears similarities to the depth of sulcus perivascular lesion in CTE but is not a diagnostic feature (3, 7). While perivascular CTE lesions may include p-tau-positive astrocytes, overlapping ARTAG pathology observed in this study was predominantly confined to the subpial surface at the depth of the cortical sulcus and was visually distinct from the CTE neuropathologic lesion. Importantly, neuronal pathology in CTE is directly related to years of exposure to RHI, whereas ARTAG pathology is not related to RHI exposure and is age-related (21). In a community-based aging cohort, Forrest et al (21) found ARTAG on neuropathological examination of 117 out of 310 individuals (38%) ranging in age from 76 to 91 (mean = 83 ± 3 years) and no instances of CTE, further supporting ARTAG as an age-related, non-RHI-related pathologic feature.

RHI exposure has been associated with several neurodegenerative pathologies, including β -amyloid deposition and Lewy body disease (22–24). Additionally, subpial TSA and perivascular astrocytic tau pathology have been reported after head trauma in several case reports (1, 25–27). It has been proposed that ARTAG, specifically subpial TSA, is associated with exposure to serum proteins and other peripherally circulating factors as a result of blood-brain barrier (BBB) dysfunction with age. BBB disruption is altered after RHI and might be exacerbated by CTE pathology (28). In this study, 69% of the RHI-exposed brain donors displayed subpial TSA, however, no association was found between subpial TSA, CTE severity, or RHI exposure. Comparison of an RHI-exposed group to an age-matched non-RHI control group is necessary to directly determine the effect of RHI exposure and CTE on the presence of ARTAG. The data presented here do not support ARTAG as a diagnostic feature of RHI exposure or CTE, consistent with the existing NINDS/NIBIB consensus criteria (3). Overall, the current study demonstrates that p-tau containing astrocytes are observed in CTE, yet are not numerous, and are associated with age not CTE severity. While the driving factor for astrocytic p-tau in CTE is age, astrocytic degeneration likely plays a role in the pathobiology and progression of CTE pathology along with other factors such as cellular senescence, BBB breakdown, and increases in baseline inflammation as features of normal aging (6).

Much of the discrepancy in previous studies regarding the role of astrocytic p-tau in CTE pathology can be attributed to examination of a narrow or limited older age range of individuals with extensive comorbid neurodegenerative diseases and reliance on cellular morphology to discriminate p-tau in astrocytes from p-tau in neurons (11). The inclusion of cases with extensive overlapping disease makes identification of a CTE-specific features challenging. The strengths of the current study are the inclusion of a large number of individuals without neuropathological evidence of comorbid disease from a wide range of ages (21–80 years old), and the use of quantitative mIF to determine cell type.

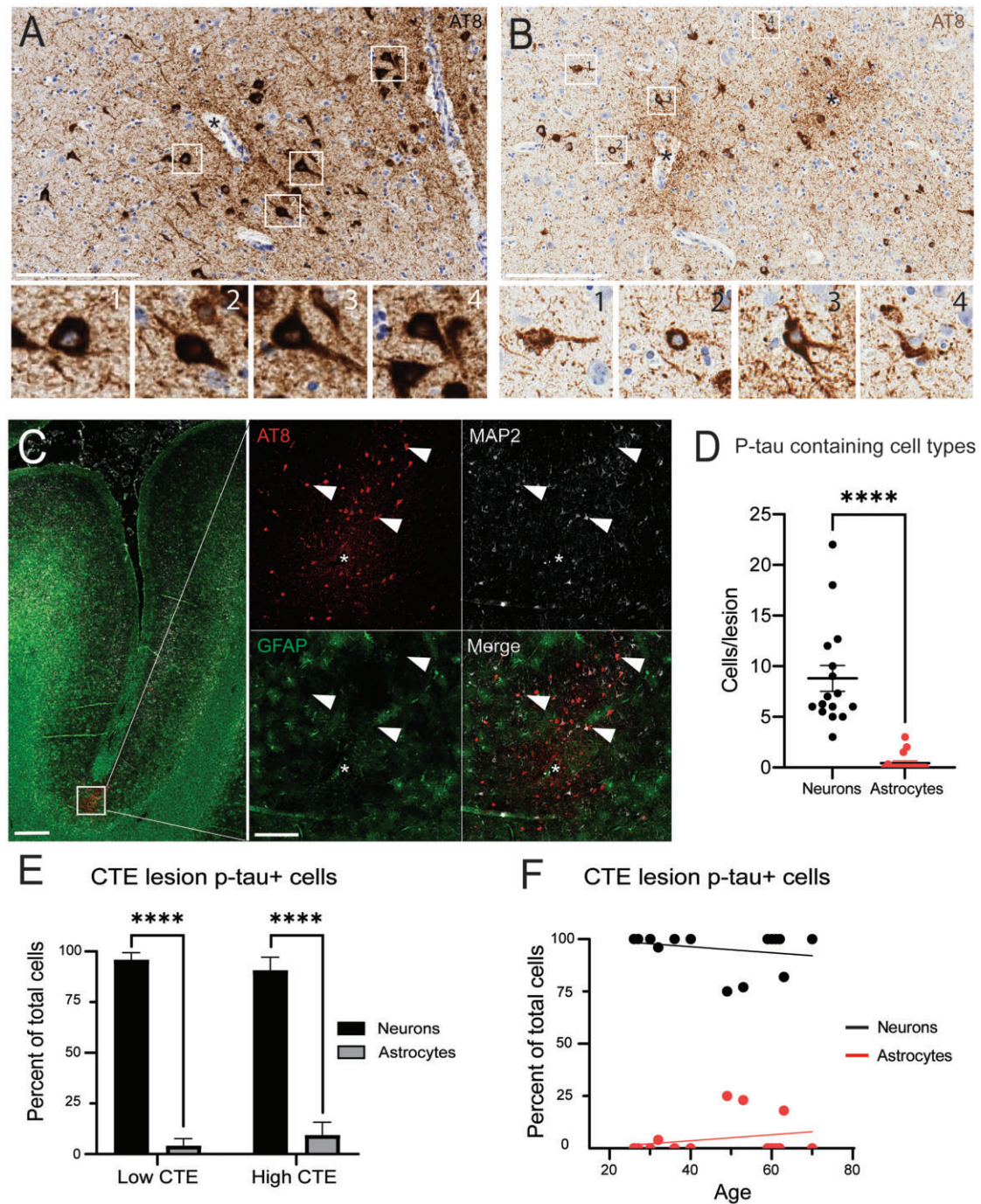


FIGURE 3. Neuronal tau defines the CTE perivascular lesion. **(A, B)** Representative brightfield images from young donors demonstrating consistent identification of neuronal p-tau at the CTE pathognomonic lesion. The CTE Brain Bank **(A)** and Australian Sports Brain Bank **(B)** both demonstrate the appearance of p-tau found around the CTE neuropathologic lesion in young individuals is primarily neuronal. **(B)** Panel is included as a representative image only and not included in the quantitative analysis with the goal of demonstrating the CTE lesion appears consistent across separate brain banks. Inserts shows a magnified view on individual neurofibrillary tangles from numbered inset boxes. Scale bar = 200 μ m. **(C)** Representative image of an immunofluorescence labeled section with CTE pathognomonic lesion at the depth of the cortical sulcus. White box indicates right panel inset zoom of the lesion. White arrows indicate neuronal p-tau co-labeled with MAP2 and AT8, asterisks indicate a blood vessel at the center of the lesion, and scale bar = 1 mm, 250 μ m, n = 17 individuals. **(D)** Quantification of total cells per CTE lesion demonstrating neuronal predominance (p < 0.0001). **(E)** In both low and high CTE, neurons represented significantly more (p < 0.0001) of the total p-tau containing cells in a lesion compared to astrocytes. Statistics generated using paired t-tests. **(F)** Neither neuronal or astrocytic p-tau was significantly associated with age within the pathognomonic lesion (p = 0.34).

Limitations

This was a convenience sample limited to brain donors neuropathologically diagnosed with CTE that is not representative of the general population. Additionally, only 2 cell-type markers were used, MAP2 and GFAP, which might not have captured all neurons or astrocytes in the tissue samples, as, for example, astrocytes are known to change their expression of GFAP in disease (29). For the CTE lesion analysis, as p-tau pathology becomes more severe, the confluent nature of p-tau distribution at end-stage disease makes it difficult to identify clearly defined lesion borders. It is possible that some lesions were missed in very severe cases of CTE in older individuals. However, this would represent only a small fraction of the cases used in the current study and is unlikely to affect the results. A larger sample of CTE lesions may reveal an association of increased perivascular astrocytes with age. Future work with additional neuronal or astrocytic markers would be useful to identify possible additional p-tau containing cellular subtypes. Furthermore, the goal of this study was to characterize the progression of p-tau pathology in CTE; therefore, healthy aged controls and RHI with no disease controls were not included. Future studies are needed to determine how the cell type profile of neuronal and astrocytic p-tau might change across all control and non-CTE, comorbid neurodegenerative disease conditions.

Conclusion

This study demonstrates, through the use of a large group of brain donors neuropathologically diagnosed with CTE, across a wide range of age at death and CTE stage, without comorbid neuropathology, that the primary p-tau containing cell type in CTE is neuronal, and that the presence of astrocytic p-tau is a factor of age, not CTE severity or years of exposure to RHI. This work provides additional evidence that CTE p-tau pathology evolves over the lifespan. Overall, this work validates the recent observations and consensus statements made by the NINDS/NIBIB consensus panels on CTE and provides a better understanding of the pathobiology of CTE as a basis for future diagnostic and therapeutic strategies.

ACKNOWLEDGMENTS

We would like to thank the clinical and neuropathology research staff at the BU CTE Center, VA Boston Healthcare System and Edith Nourse Rogers VA Medical Center, and Dr. Michael E. Buckland for the contribution of tissue from the Australian Sports Brain Bank.

REFERENCES

- McKee AC, Stern RA, Nowinski CJ, et al. The spectrum of disease in chronic traumatic encephalopathy. *Brain* 2013;136:43–64
- Mez J, Daneshvar DH, Abdolmohammadi B, et al. Duration of American football play and chronic traumatic encephalopathy. *Ann Neurol* 2020;87:116–31
- Bieniek KF, Cairns NJ, Crary JF, et al.; TBI/CTE Research Group. The second NINDS/NIBIB consensus meeting to define neuropathological criteria for the diagnosis of chronic traumatic encephalopathy. *J Neuropathol Exp Neurol* 2021;80:210–9
- McKee AC, Cairns NJ, Dickson DW, et al.; TBI/CTE group. The first NINDS/NIBIB consensus meeting to define neuropathological criteria for the diagnosis of chronic traumatic encephalopathy. *Acta Neuropathol* 2016;131:75–86
- Mez J, Alosco ML, Daneshvar DH, et al. Validity of the 2014 traumatic encephalopathy syndrome criteria for CTE pathology. *Alzheimers Dement* 2021;17:1709–24
- Cherry JD, Kim SH, Stein TD, et al. Evolution of neuronal and glial tau isoforms in chronic traumatic encephalopathy. *Brain Pathol* 2020;30:913–25
- Kovacs GG, Ferrer I, Grinberg LT, et al. Aging-related tau astroglial pathology (ARTAG): Harmonized evaluation strategy. *Acta Neuropathol* 2016;131:87–102
- Kovacs GG. Astroglia and tau: New perspectives. *Front Aging Neurosci* 2020;12:96
- Mattiace LA, Wu E, Aronson M, et al. A new type of neuritic plaque without amyloid in corticostriatal degeneration without achromasia. *J Neuropathol Exp Neurol* 1991;50:310
- Arena JD, Johnson VE, Lee EB, et al. Astroglial tau pathology alone preferentially concentrates at sulcal depths in chronic traumatic encephalopathy neuropathologic change. *Brain Commun* 2020;2:fcaa210
- Ameen-Ali KE, Bretzin A, Lee EB, et al.; CONNECT-TBI Investigators. Detection of astrocytic tau pathology facilitates recognition of chronic traumatic encephalopathy neuropathologic change. *Acta Neuropathol Commun* 2022;10:50
- Montine TJ, Phelps CH, Beach TG, et al.; Alzheimer's Association. National Institute on Aging-Alzheimer's Association guidelines for the neuropathologic assessment of Alzheimer's disease: A practical approach. *Acta Neuropathol* 2012;123:1–11
- McKeith IG. Consensus guidelines for the clinical and pathologic diagnosis of dementia with Lewy bodies (DLB): Report of the Consortium on DLB International Workshop. *J Alzheimers Dis* 2006;9:417–23
- Mackenzie IR, Neumann M, Bigio EH, et al. Nomenclature and nosology for neuropathologic subtypes of frontotemporal lobar degeneration: An update. *Acta Neuropathol* 2010;119:1–4
- Love S, Louis DN, Ellison DW. *Greenfield's Neuropathology, Two-Volume Set*. 8th edn. Boca Raton, FL: CRC Press 2008
- McKee AC, Cantu RC, Nowinski CJ, et al. Chronic traumatic encephalopathy in athletes: Progressive tauopathy after repetitive head injury. *J Neuropathol Exp Neurol* 2009;68:709–35
- Stern RA, Daneshvar DH, Baugh CM, et al. Clinical presentation of chronic traumatic encephalopathy. *Neurology* 2013;81:1122–9
- Cherry JD, Tripodis Y, Alvarez VE, et al. Microglial neuroinflammation contributes to tau accumulation in chronic traumatic encephalopathy. *Acta Neuropathol Commun* 2016;4:112
- Cherry JD, Esnault CD, Baucom ZH, et al. Tau isoforms are differentially expressed across the hippocampus in chronic traumatic encephalopathy and Alzheimer's disease. *Acta Neuropathol Commun* 2021;9:86
- Armstrong RA, McKee AC, Stein TD, et al. A quantitative study of tau pathology in eleven cases of chronic traumatic encephalopathy. *Neuropathol Appl Neurobiol* 2017;43:154–166
- Forrest SL, Kril JJ, Wagner S, et al. Chronic traumatic encephalopathy (CTE) is absent from a European community-based aging cohort while cortical aging-related tau astroglial pathology (ARTAG) is highly prevalent. *J Neuropathol Exp Neurol* 2019;78:398–405
- Stein TD, Montenegro PH, Alvarez VE, et al. Beta-amyloid deposition in chronic traumatic encephalopathy. *Acta Neuropathol* 2015;130:21–34
- Adams JW, Alosco ML, Mez J, et al. Association of probable REM sleep behavior disorder with pathology and years of contact sports play in chronic traumatic encephalopathy. *Acta Neuropathol* 2020;140:851–62
- Adams JW, Alvarez VE, Mez J, et al. Lewy body pathology and chronic traumatic encephalopathy associated with contact sports. *J Neuropathol Exp Neurol* 2018;77:757–68
- Goldfinger MH, Ling H, Tilley BS, et al. The aftermath of boxing revisited: Identifying chronic traumatic encephalopathy pathology in the original Corsellis boxer series. *Acta Neuropathol* 2018;136:973–4
- Shively SB, Horkayne-Szakaly I, Jones RV, et al. Characterisation of interface astroglial scarring in the human brain after blast exposure: A post-mortem case series. *Lancet Neurol* 2016;15:944–53
- Bachstetter AD, Garrett FG, Jicha GA, et al. Space-occupying brain lesions, trauma-related tau astroglial pathology, and ARTAG: A report of two cases and a literature review. *Acta Neuropathol Commun* 2021;9:49
- Doherty CP, O'Keefe E, Wallace E, et al. Blood-brain barrier dysfunction as a hallmark pathology in chronic traumatic encephalopathy. *J Neuropathol Exp Neurol* 2016;75:656–62
- Escartin C, Galea E, Lakatos A, et al. Reactive astrocyte nomenclature, definitions, and future directions. *Nat Neurosci* 2021;24:312–325